



## Hybrid hydroxyapatite/graphene oxide composites materials synthesized from eggshell for adsorption of Cr(VI) in aqueous solution

Rui Wu, Huizhong Wu, Yingxi Wang\*, Ling Li\*

Ministry of Education Key Laboratory for Synthesis and Application of Organic Function Molecules, Hubei University 430062, China, emails: 16890202@qq.com (Y. Wang), lingli@hubu.edu.cn (L. Li), 2363565966@qq.com (R. Wu), 2367355465@qq.com (H. Wu)

Received 23 April 2022; Accepted 11 November 2022

### ABSTRACT

In this work, hydroxyapatite/graphene oxide hybrid composites (HAP/GO) were prepared from eggshell by solvothermal method, which was mainly used as adsorbents for Cr(VI) removal in wastewater. The effect of graphene oxide (GO) on the structure and removal efficiency of HAP/GO was discussed. The results showed that the Cr(VI) removal of HAP/GO<sub>10%</sub> can reach more than 90% within 1 h, and the adsorption conforms to the first-order kinetics. It was found that the addition of GO changed the pore size distribution of HAP/GO and improved Cr(VI) removal. It can be concluded that the swelling of GO in aqueous solution leads to an increase in the interaction between the dissociated carboxyl groups and Cr(VI), thereby improving the adsorption efficiency.

*Keywords:* Composite materials; Hydroxyapatite; Graphene oxide; Adsorption; Chromium(VI)

### 1. Introduction

Soil and groundwater are key components in the sustainable management of the subsurface environment [1]. Chromium is a silver white hard metal, mainly in the form of metal chromium, chromate. It is one of the most useful and dangerous materials and has been widely used in metal and chemical industries, such as steel, chemical, leather, textile manufacturing and electroplating [2–4]. Chromium metal ions have various valence states. Trivalent chromium is an essential trace element for human body, which is closely related to lipid metabolism, while hexavalent chromium has strong mutagenicity and carcinogenicity. Hexavalent chromium is an ingestive or inhalation toxicant, and its toxicity is 100 times higher than that of trivalent chromium [5]. It is a carcinogen released by the International Center for Anticancer Research and the United States Toxicological Organization [6]. It can convert haemoglobin into methaemoglobin and disturb the oxidation, reduction and hydrolysis process in vivo [7]. Hexavalent chromium has a strong

damage to the skin, skin contact with hexavalent chromium will appear dermatitis and eczema and other allergic reactions. The residual hexavalent chromium in the leather can be absorbed through the skin and respiratory tract, causing damage to the stomach, liver and kidney functions, and may also hurt the eyes, resulting in retinal haemorrhage, optic atrophy and other adverse consequences [8].

According to relevant regulations, the hexavalent chromium content in industrial effluent cannot exceed 0.5 mg/L. Since 2008, the motor electronic equipment shall not contain hexavalent chromium [9]. In the test of heavy metal ions in related sewage [10]. As for the metal hexavalent chromium content is not more than 0.1 mg/kg. The content of hexavalent chromium in leather cannot exceed 3 mg/kg [11–13]. It can also be seen from these provisions that hexavalent chromium is not uncommon in life and is used in many industrial products.

In recent years, both domestic and foreign, for hexavalent chromium emission standards are very strict. The reason for this limitation is that hexavalent chromium is an extremely

\* Corresponding authors

toxic substance [14–16]. If hexavalent chromium is contained in water, the impact on human beings, livestock and crops is great. Many methods have been developed for hexavalent chromium ion treatment, among which liquid–liquid extraction method, chemical precipitation method, reverse osmosis method and dialysis method are chromium removal [17]. Adsorption method is an ideal method with high efficiency and low cost for removing Cr(VI). In recent years, the adsorption technology of toxic metal ions and the design and synthesis of new adsorbents have attracted wide attention. Several adsorbents for removing Cr(VI) were developed. However, most studies on adsorbents are only based on academic interest. In fact, biocompatibility will make this material have practical application value [18].

Hydroxyapatite is a promising adsorbent material. It has special crystal chemical characteristics, good ion exchange performance, and can treat heavy metal ions and organic polymer pollutants in industrial wastewater [19]. It has a wide range of metal ions and good coordination with the environment not cause secondary pollution [20]. However, the adsorption capacity is limited. To improve the adsorption capacity of hydroxyapatite (HAP), it is necessary to design composites based on HAP. Because of the hydrophilic character, graphite oxide (GO) can be easily dispersed in water and other polar solvents, and GO can also be used as an adsorbent. Furthermore, the hydrophilic functional groups make graphene oxide easy to hybridize with other materials to form composites with a single layer structure and excellent specific surface area, resulting in considerable adsorption capacity [21]. The formation of hydroxyapatite/graphene oxide hybrid composites (HAP/GO) composite is expected to improve the adsorption capacity of Cr(VI).

Among kinds of synthesis of HAP, the calcium source is usually calcium carbonate, which is expensive to apply to wastewater treatment. Reducing the synthesis cost is expected to broaden the application scope of HAP. In the food industry, eggs are processed in a large amount, and

many eggshells need to be processed every day. For example, a factory that processes 100,000 tons of eggs annually produces about 13,000 tons of eggshells. On average, there are dozens of tons per day. Not only are these eggshells ineffective, they also cost money to dispose of. The main component of eggshells is calcium carbonate, which is as high as 96%. Therefore, choosing eggshells as calcium sources and converting them into products for wastewater treatment is expected to explore the commercial value of eggshells.

Inspired by this, eggshell was selected as calcium source to prepare HAP/GO, as shown in Fig. 1. The formation of HAP/GO composite is expected to improve the adsorption capacity of Cr(VI). The adsorption of Cr(VI) on HAP/GO was synthesized. The synthesis and adsorption of HAP/GO are shown in Fig. 1.

## 2. Experimental section

### 2.1. Chemicals, materials and instruments

The eggshells are collected in the school cafeteria. After cleaning, the inner membrane of the eggshells is carefully peeled off. After drying at 60°C for 48 h, the eggshells are ground into powder in a mill for use. Graphite (Aladdin, analytically pure),  $\text{NaNO}_3$ , concentrated sulfuric acid,  $\text{KMnO}_4$ ,  $\text{H}_2\text{O}_2$ ,  $\text{NH}_4\text{H}_2\text{PO}_4$ , anhydrous ethanol, dibenzoylhydrazine, acetone, ethylenediaminetetraacetic acid (EDTA), phosphoric acid,  $\text{K}_2\text{CrO}_4$  are all National Pharmaceutical Factory, analytically pure.

500 mL three-necking flask, 100 mL constant pressure dropping funnel, 100°C mercury thermometer, sand core funnel, electronic balance, 85-2 type constant temperature magnetic agitator (Shanghai Sile Instrument Co., Ltd., Shanghai), DF-101S collector constant temperature heating magnetic agitator (Henan Gongyi Yuhua Instrument Co., Ltd., Henan), 800B type centrifuge (Shanghai Anting Scientific Instrument Factory, Shanghai), ultrasonic cleaning machine (Kunshan

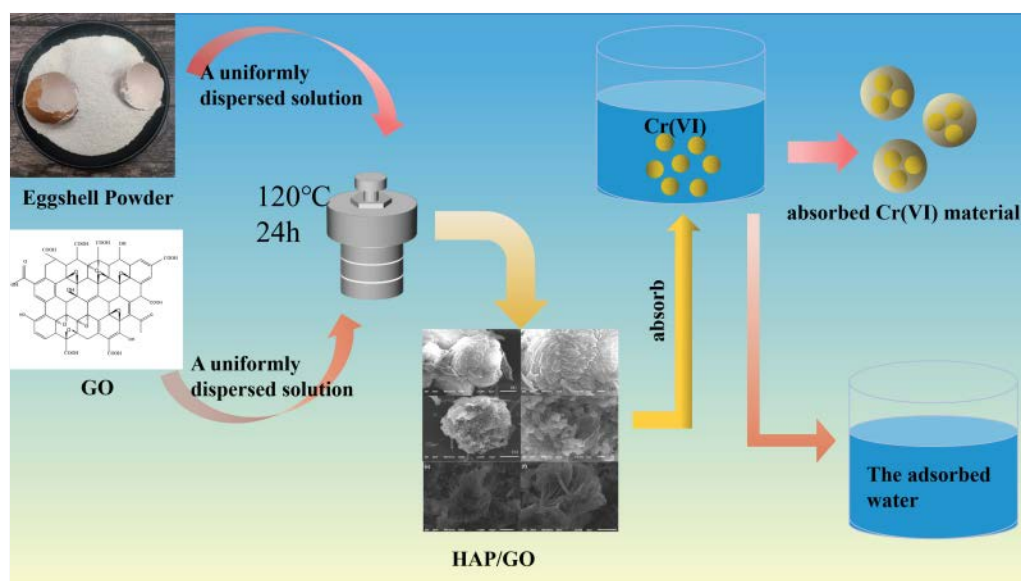


Fig. 1. Synthesis and adsorption of HAP/GO.

Ultrasonic Instruments Co., Ltd., Kunshan), 101-A type of electrothermal blowing (Beijing Everlasting Light Medical Instrument Factory, Beijing), ultraviolet-visible spectrophotometer (Shanghai Instrument Analysis Instrument Co., Ltd., Shanghai), SHZ-D (III) circulating water vacuum pump (Henan Gongyi City Instrument Co., Ltd., Henan, China (Guohua Electric Co., Ltd., China)), speed control multi-purpose oscillator (Guohua Electric Co., Ltd., China).

## 2.2. Synthesis of materials

### 2.2.1. Synthesis of GO

There are some modifications to the method of preparing GO according to the literature [22]. The specific method is as follows: 0.5 g graphite, 0.5 g  $\text{NaNO}_3$  are added to a three-necked flask, 23 mL concentrated  $\text{H}_2\text{SO}_4$  is slowly added, ice bath ( $0^\circ\text{C} \pm 5^\circ\text{C}$ ), magnetic stirring for 15 min, while slowly adding 4 g  $\text{KMnO}_4$ ,  $35^\circ\text{C} \pm 5^\circ\text{C}$  water bath, stirring for 2 h, slowly adding 40 mL water, transferring to  $90^\circ\text{C} \pm 5^\circ\text{C}$  oil bath, stirring for 1 h; adding 100 mL water, 3 mL  $\text{H}_2\text{O}_2$ , stirring for 1–2 min, stop the reaction and filter with sand while it is hot. After suction filtration, add about 100 mL to disperse the precipitate in water centrifuge. After centrifugation, discard the supernatant, remove the bottom precipitate, place it in a watch glass, and put it in an oven 48 h, the temperature is controlled at  $60^\circ\text{C}$ .

### 2.2.2. Synthesis of HAP

25 mL of 0.1 g/mL  $\text{NH}_4\text{H}_2\text{PO}_4$  was added to 0.3 g of eggshell powder and placed in a polytetrafluoroethylene reactor, and reacted at  $120^\circ\text{C}$  for 24 h. After the reaction is completed, the product is alternately filtered with distilled water and absolute ethanol. Finally, it was dried in an oven at  $60^\circ\text{C}$  for 24 h.

### 2.2.3. Synthesis of hybrid material HAP/GO

0.05 g graphene oxide (GO) was dispersed in 25 mL of 0.1 g/mL  $\text{NH}_4\text{H}_2\text{PO}_4$ , and 0.3 g eggshell powder was added and placed in a polytetrafluoroethylene reactor at  $120^\circ\text{C}$  for 24 h, respectively. After the reaction was completed, the product was filtered alternately with distilled water and anhydrous ethanol, and finally dried in an oven at  $60^\circ\text{C}$  for 24 h.

## 2.3. Characterization

The HAP and hybrid materials GO/HAP were characterized by X-ray diffraction (XRD), infrared and SEM.D/max-III C X-ray diffractometer (Shimadzu Corporation, Japan). Single-frequency infrared spectrophotometer (PerkinElmer, USA) EPMA-8705QH2 scanning electron microscope (Shimadzu Corporation, Japan).

## 2.4. Determination of Cr(VI) concentration

0.2 g of diphenylcarbazide was weighed, dissolved in 50 mL of acetone, and transferred into a 100 mL volumetric flask. Add 1% of EDTA 2.5 mL to the above solution,

evenly mixed and stored in a brown bottle refrigerator. Mixing agent: respectively configure 1:1 sulfuric acid and 1:1 phosphoric acid, and then mix the two in equal volume. The reference experiment procedure is the same as the "Water and Wastewater Monitoring and Analysis Method" of the National Environmental Protection Agency. Several 50 mL colorimetric tubes were added with 100 mg/L Cr(VI) standard solution of 0.00, 0.20, 0.50, 1.00, 2.00, 4.00, 6.00, 8.00, and 10.00 mL, respectively. The tubes were diluted with water to the standard line and shaken evenly with 1 mL mixed acid. Then 2 mL chromogenic agent was added and shaken evenly with a plug. Place 10 min colorimetric dish, at 540 wavelength, with water as reference, determination of absorbance A.

## 2.5. Comparison of the adsorption properties of HAP and HAP/GO hybrid materials for Cr(VI)

Prepare Cr(VI) solutions with concentrations of 4.0, 3.5, 3.0, 2.5, 2.0, 1.5, 1.0, and 0.5 mg/L, respectively. Take two 4 mL portions for each group of different concentrations; divide into two groups, one group is added with 0.01 g of hydroxyapatite, and the other group is added with 0.01 g of graphene oxide and hydroxyapatite hybrid material. Then, the sixteen groups of solution were placed in oscillation for an hour, centrifuged, each group of solution 2 mL supernatant, diluted to 25 mL with water, and then added 1 mL mixed acid, and then added 2 mL display agent. Finally, standing for 10 min, with water as the reference, the absorbance was measured and recorded at 540 nm.

## 2.6. Discussion on isothermal adsorption mode

Add 50 mL of Cr(VI) with a concentration of 3.0 mg/L to two 100 mL Erlenmeyer flasks, then add 0.2 g HAP material and HAP/GO hybrid material, magnetically stir, take out 4 mL centrifugation every 10 min After centrifugation, take out 2 mL of the supernatant, dilute to a constant volume of 25 mL, add 1 mL of mixed acid, and then add 2 mL of color reagent, close the plug and shake to measure its absorbance. During the whole process, the temperature of the solution is controlled at  $19^\circ\text{C}$ . Process the experimental data and explore its isotherm adsorption mode.

## 2.7. Relationship between HAP/GO adsorption of Cr(VI) ion and time

Put 0.01 g of graphene oxide and hydroxyapatite hybrid material into the reagent bottle, and then add 4 mL of 3 mg/L Cr(VI) solution. Prepare six parts of the above solution and place them in a shaker to oscillate at the same time. A reagent bottle was taken out every 10 min, and the supernatant was taken out and centrifuged. Then, 2 mL of the supernatant after centrifugation was taken and put into a colorimetric dish for further use. When the six test bottles were taken out, the six colorimetric dishes were put into 2 mL liquid, and the distilled water was added to the six test bottles to dilute 25 mL, then 1 mL mixed acid was added, and 2 mL chromogenic agent was added. Finally, standing for 10 min, with water as the reference, the absorbance was measured and recorded.

### 3. Result and discussion

#### 3.1. Characterization

The XRD characterization of HAP and HAP/GO is shown in Fig. 2a. The characteristic diffraction peaks of HAP are consistent with those reported in the literature, indicating that HAP was successfully synthesized from eggshells. The characteristic diffraction peaks of HAP are completely retained in HAP/GO, indicating that the basic crystal structure of HAP may still be retained in the hybrid material. However, the characteristic diffraction peaks of HAP and HAP/GO are different at small angles. HAP/GO has a slight difference between 10% and 20%, indicating that the addition of GO has a certain effect on the structure.

The infrared characterization of HAP/GO is shown in Fig. 2b. In the infrared spectrum of HAP, the characteristic vibration peaks at 3,570 and 634  $\text{cm}^{-1}$  are the characteristic absorption peaks of  $-\text{OH}$ , and the characteristic absorption peaks of  $\text{PO}_4^{3-}$  at 1,095; 963 and 603  $\text{cm}^{-1}$  are the characteristic absorption peaks of  $\text{PO}_4^{3-}$ . Therefore, it is further proved that the basic structure of HAP is retained in HAP/GO. However, HAP/GO is significantly different between 4,000 and 3,000  $\text{cm}^{-1}$ , which further confirms that the addition of GO has a certain influence on the structure. And, the higher the content of GO, the red shift of the characteristic peaks in this area to a great extent. It is worth noting that GO has a characteristic absorption peak at 1,703  $\text{cm}^{-1}$ , which belongs to the  $-\text{COOH}$  of GO, but the characteristic peak here is difficult to observe in HAP/GO. It is inferred that the reason may be due to the  $-\text{COOH}$  and  $-\text{COOH}$  in GO. The  $-\text{COOH}$  in HAP has an effect.

The surface condition of HAP and hybrid material HAP/GO observed by scanning electron microscope (SEM) is shown in Fig. 3. The shape characteristics of HAP and HAP/GO are completely different, which shows that the hybrid materials HAP and GO are not only a blend of two materials, but a new material. In HAP/GO with GO content of 10%, the basic lamellar structure of HAP was

still visible, but it was almost clustered together to form closely packed flower clusters. HAP/GO with 20% GO content is also the flower cluster structure, but it obviously loses the characteristic long sheet or long fibrous structure of HAP, like some closely packed scales, which is different from HAP structure. This indicated that when the GO content was too high, GO would aggregate in the hybrid. Therefore, HAP/GO<sub>10%</sub> was selected for subsequent experiments.

#### 3.2. Comparison of adsorption performance between HAP and HAP/GO

The adsorption capacity of HAP and HAP/GO for different concentrations of Cr(VI) were compared. The removal rate of Cr(VI) is shown in Fig. 4 which shows that the removal rate of HAP and HAP/GO is very high in a short period of time, but it can be seen that the adsorption capacity of HAP/GO is higher than that of HAP regardless of the concentration (Fig. 5). It can be seen that when the initial concentration of Cr(VI) is 0.5 and 3.0 mg/L, the adsorption rate of HAP and HAP/GO for Cr(VI) differs the most. This indicates that HAP/GO has better adsorption performance than HAP, especially when the concentration is 0.5 and 3.0 mg/L. Therefore, compared with HAP, HAP/GO can be used as a better adsorbent to treat chromium-containing wastewater. Therefore, the concentration of 3.0 mg/L was selected for the experiment.

Fig. 4b shows the adsorption capacity of HAP and hybrid material HAP/GO on Cr(VI) at different times at a temperature of 19°C. Observing Fig. 6, it can be found from Fig. 5 that the adsorption rate of chromium ions increases with the increase of time when it is measured every within 1 h. The longer the adsorption time was, the greater the difference between the adsorption rate of GO/HAP hybrid materials and that of HAP was. It can be seen that at the same concentration of chromium-containing wastewater, the longer the adsorption time, the greater the adsorption advantage of GO/HAP

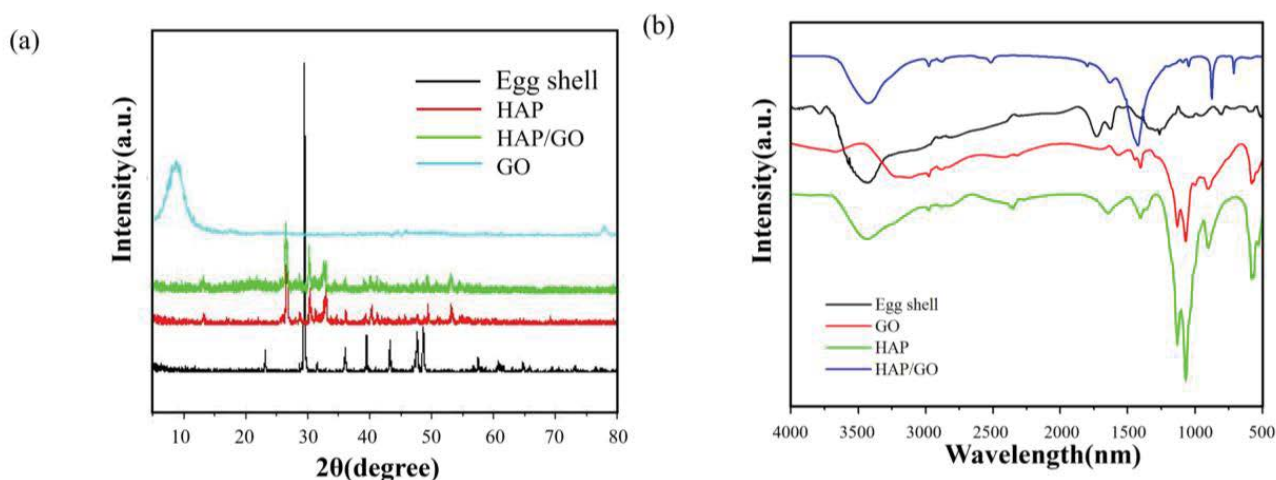


Fig. 2. (a) XRD patterns of eggshell, GO, HAP and HAP/GO, (b) infrared patterns of eggshell, GO, HAP and HAP/GO.

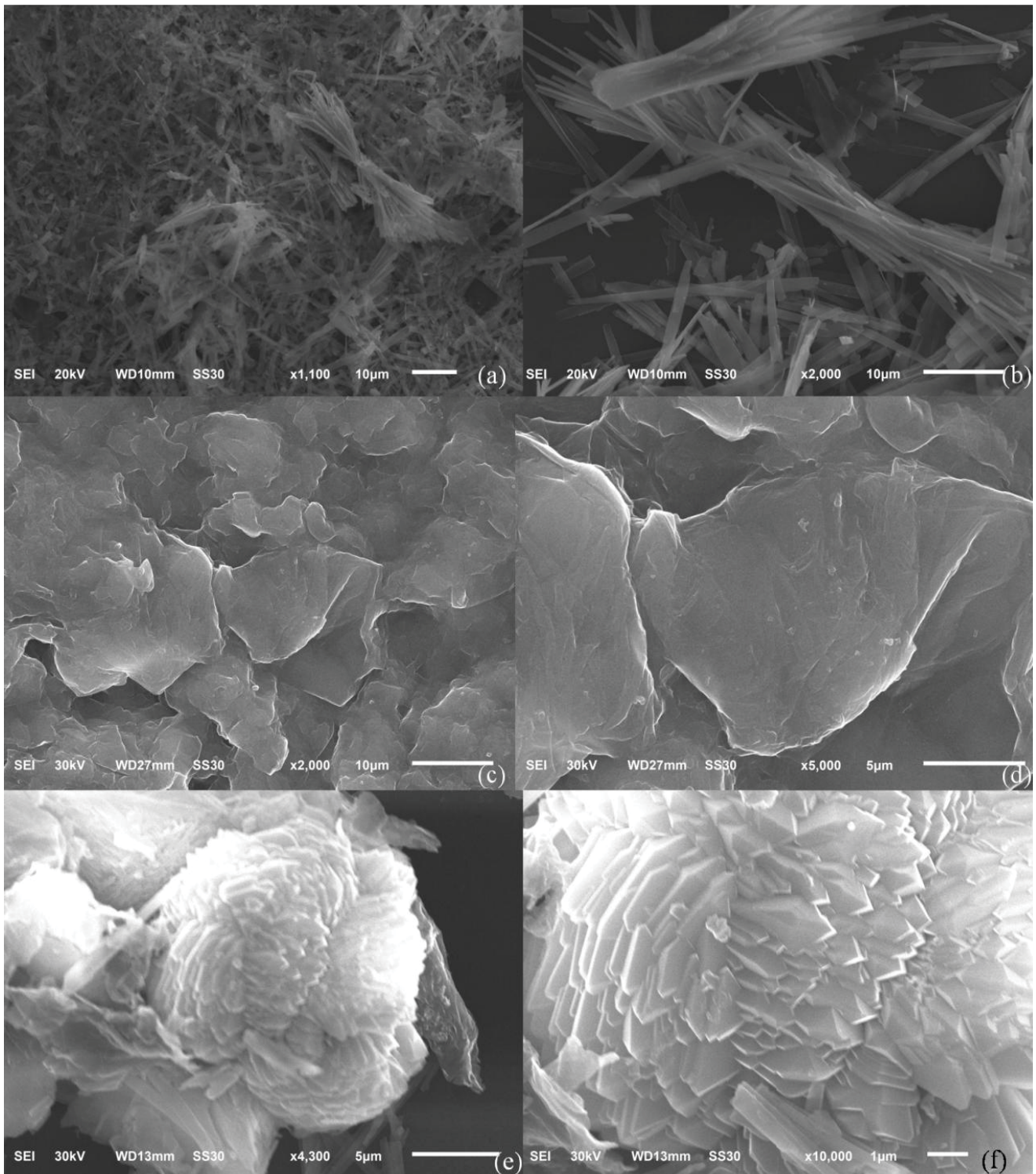


Fig. 3. SEM of (a,b) HAP, (c,d) HAP/GO<sub>20%</sub> and (e,f) HAP/GO<sub>10%</sub>.

material relative to HAP. In addition to the low cost of synthesis, the adsorption performance for Cr(VI) is better than other reported adsorbents, as shown in Table 1. As shown in Table 1, the materials we use are cheaper

than those reported in other literature. The adsorption performance of the material reported in this study is also better than that of Cr(VI) reported in other literatures.

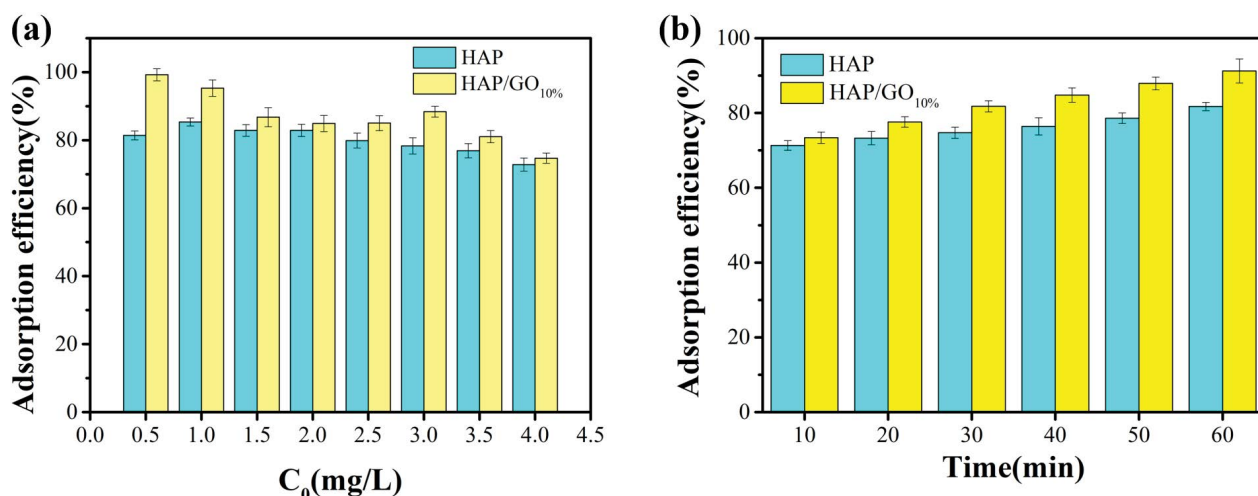


Fig. 4. (a) Comparison of the adsorption performance of HAP and HAP/GO on different concentrations of chromium-containing wastewater. The amount of HAP is 0.01 g; the amount of GO/HAP is 0.01 g and (b) the adsorption capacity of the hybrid material HAP/GO with different concentrations of chromium-containing wastewater.

Table 1  
Comparison of the Cr(VI) adsorption of various adsorbent materials

Adsorbent	Adsorption rate	References
Goethite	78.5%	[23]
Functionalized polyimide fibers	60.44%–89.29%	[24]
Nanoporous anodized alumina (AAO)	82%	[25]
Cynodon dactylon plant-mediated amino-grouped silica-layered magnetic nanoadsorbent	60.6%	[26]
HAP/GO	More than 90%	This work

### 3.3. Isothermal adsorption models

In order to describe the adsorption process more scientifically, Freundlich model and Langmuir model [27] were selected for adsorption. The Freundlich equation is:

$$Q_e = K_F C_e^{1/n} \tag{1}$$

where  $K_F$  and  $1/n$  represent Freundlich adsorption capacity coefficient and adsorption intensity coefficient, respectively. Fig. 5a shows the linear relationship between  $\ln Q_e$  and  $\ln C_e$  in this model.

The Langmuir adsorption isotherm model has been successfully applied to many wastewater adsorption processes [28]. Expressed as an equation:

$$Q_e = \frac{Q_0 K_L C_e}{1 + K_L C_e} \tag{2}$$

where  $Q_e$ : the equilibrium adsorption capacity of hexavalent chromium ions on the adsorbent (mg/g);  $C_e$ : the concentration of Cr(VI) in the solution when the adsorption reaches equilibrium (mg/L);  $Q_0$ : the maximum adsorption capacity of the adsorbent (mg/g);  $K_L$ : Langmuir adsorption constant (L/mg), which is related to the free energy of the adsorption

Table 2  
The simulation equations of different isothermal adsorption modes of HAP and HAP/GO

Adsorption mode	Degree of fitting	Fit curve
HAP	Freundlich	$Y = 0.71919X + 0.45149$
GO/HAP		$Y = 0.56672X + 0.56908$
HAP	Langmuir	$Y = 0.38968X + 0.32036$
GO/HAP		$Y = 0.5045X + 0.14788$

process. Fig. 5a shows the linear relationship between  $(C_e/Q_e)$  and  $C_e$ .

The simulation equations and fitting coefficients of the two isothermal adsorption modes are shown in Table 2. It can be seen from Fig. 4 that both HAP and HAP/GO are more in line with the Freundlich isotherm adsorption model.

### 3.4. Adsorption kinetics study

According to the measured Cr(VI) concentration, the adsorption performance can be calculated and evaluated according to the following formula. The calculation

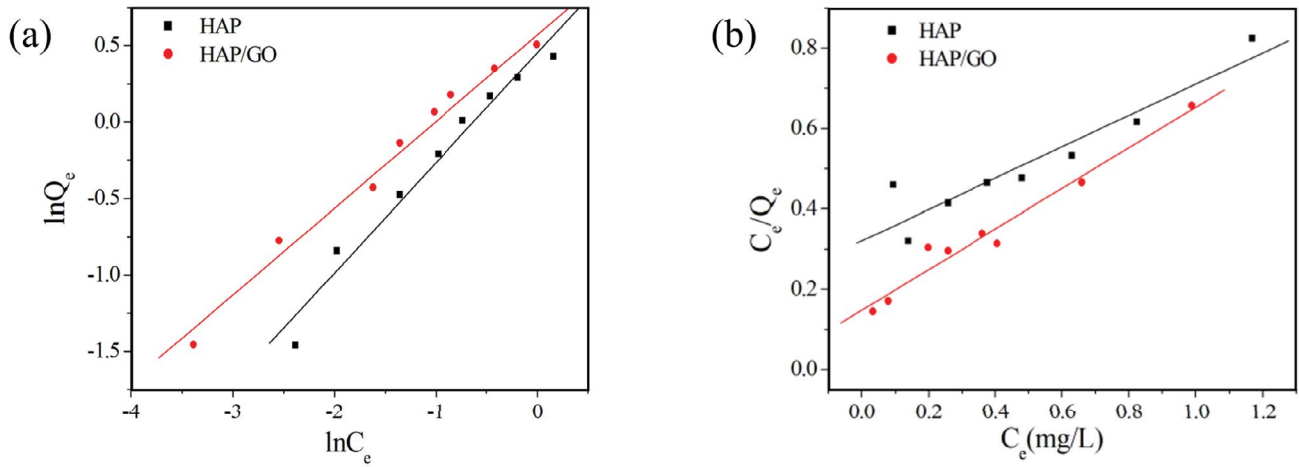


Fig. 5. (a) Freundlich adsorption isotherm simulation of Cr(VI) by HAP and HAP/GO and (b) Langmuir adsorption isotherm simulation of Cr(VI) by HAP and HAP/GO.

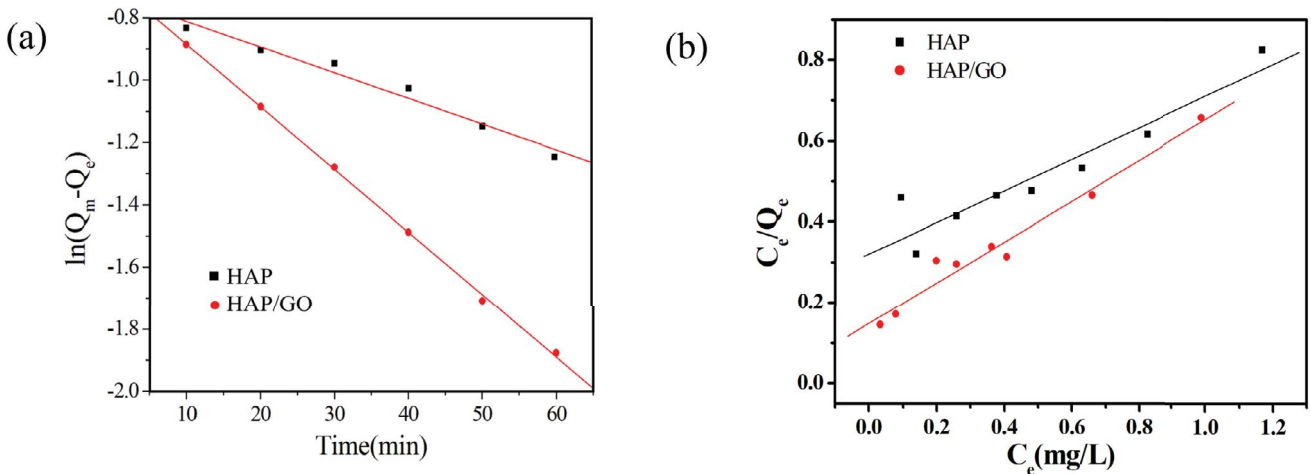


Fig. 6. (a) First-order kinetic simulation of Cr(VI) adsorption by HAP and HAP/GO hybrid materials and (b) the second-order kinetic simulation of Cr(VI) adsorption by HAP and HAP/GO hybrid materials.

formula for the adsorption capacity ( $Q_e$ ) of HAP and hybrid material HAP/GO is as follows:

$$Q_e = \left[ \frac{(c_i - c_e)}{m} \right] \times V \tag{3}$$

where  $c_i$  and  $c_e$  are the initial concentration of potassium dichromate solution and the concentration after adsorption equilibrium, respectively, in mg/L,  $m$  is the mass of HAP and hybrid material HAP/GO, in g;  $V$  is the volume of the solution to be adsorbed, in L. In order to evaluate the kinetic characteristics of the adsorption process, the adsorbed Cr(VI) at different reaction times can be calculated according to the following formula:

$$Q_t = \left[ \frac{(c_e - c_t)}{m} \right] \times V \tag{4}$$

where  $c_t$  is the concentration of the Cr(VI) solution at the time when it is adsorbed, and the unit is mg/L. The adsorption performance of HAP and hybrid material HAP/GO can also be expressed by its adsorption rate  $A$  for Cr(VI):

$$A = \frac{(c_i - c_e)}{c_i} \times 100\% \tag{5}$$

In order to understand the adsorption kinetics of Cr(VI) by HAP and HAP/GO more accurately, the adsorption rate equation can be used to regress the experimental data, among which the first-order rate equation and the second-order rate equation are used to study the adsorption. The more commonly used method of the mechanism of action between agent and adsorbate [29].

The first order adsorption rate equation based on the amount of solid adsorption:

$$\log(Q_e - Q_t) = \log Q_e - \frac{k_1 t}{2.303} \tag{6}$$

The two-stage adsorption rate equation based on the amount of solid adsorption:

$$\frac{t}{Q_i} = \frac{1}{(K_2 Q_e^2)} + \frac{t}{Q_e} \tag{7}$$

Fig. 6 shows the first-order kinetics and the second-order kinetics simulation respectively. Comparing the fitting coefficients in the two tables, we can see that the adsorption of Cr(VI) by HAP conforms to the second-order kinetics, and the adsorption of Cr(VI) by the hybrid material HAP/GO conforms to the first-order kinetics. The kinetic fitting equation and fitting coefficient are shown in Table 3 It can be seen that the adsorption of Cr(VI) by HAP and HAP/GO is more in line with the second-order kinetics [30].

### 3.5. Stability and reusability of HAP/GO

In order to evaluate the reusability and stability of HAP/GO, the adsorbent efficiency and XRD patterns of HAP/GO were examined. Fig. 7 shows the continuous multi-cycle Cr(VI) adsorption using HAP/GO. After 5 cycles of non-regeneration treatment, the Cr(VI) adsorption efficiency

remained almost unchanged, indicating that HAP/GO can be used as a stable and reusable adsorbent. The decrease in Cr(VI) adsorption may be due to the loss and aggregation of HAP/GO in each cycle, and the adsorption of Cr(VI) on the surface of HAP/GO. The reused HAP/GO was also

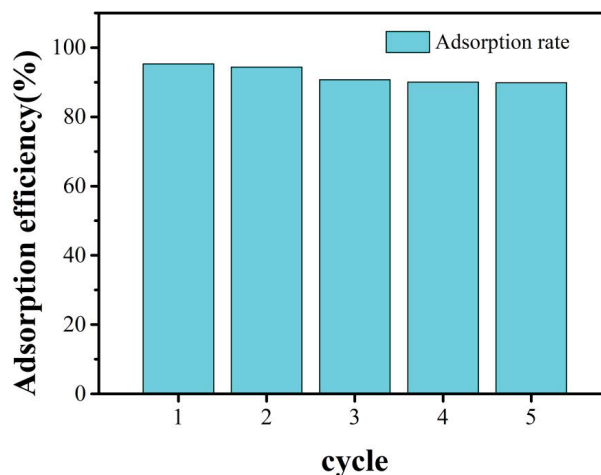


Fig. 7. Adsorption performance of HAP/GO in 5 reuse cycles had the same reaction conditions. HAP amount is 0.01 g, Cr(VI) concentration: 1.0 mg/L.

Table 3

Fitting equation of adsorption kinetics of Cr(VI) on HAP and HAP hybrid materials

Kinetic equations	Materials	Degree of fitting	Fit curve
First-order dynamics	HAP	0.9872	$Y = -0.00823X - 0.72954$
	GO/HAP	0.9996	$Y = -0.0201X - 0.68436$
Second-order dynamics	HAP	0.9989	$Y = 0.80153X + 2.18129$
	GO/HAP	0.9992	$Y = 0.70201X + 2.89566$

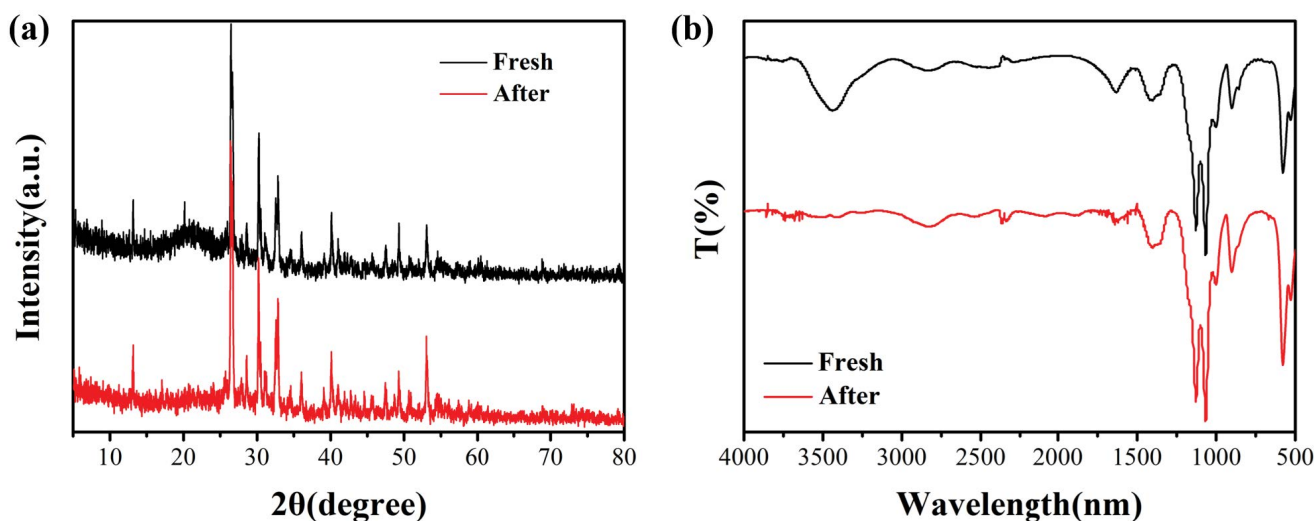


Fig. 8. XRD (a) and FT-IR (b) of the materials before and after reaction.



characterized by XRD and Fourier-transform infrared spectroscopy (FT-IR). As shown in Fig. 8a and b, the HAP/GO used has almost the same XRD pattern and FT-IR spectrum as fresh HAP/GO, indicating that HAP/GO is a stable and durable adsorbent.

#### 4. Conclusions

In this topic, graphene oxide, HAP and hybrid material HAP/GO were synthesized. By controlling the amount of adsorbent, Cr(VI) concentration and adsorption time, the adsorption mechanism of HAP and hybrid material HAP/GO on Cr(VI) was explored. Concluded as follow: First, the adsorption capacity of the hybrid material HAP/GO for Cr(VI) is stronger than the adsorption capacity of the same amount of HAP. The adsorption of Cr(VI) by hybrid material HAP/GO accords with the kinetic process and can be described by the second-order kinetic equation; Secondly, the adsorption behavior of the hybrid material HAP/GO for Cr(VI) conforms to the Freundlich model isothermal model.

#### Declaration of competing interest

The authors declare that they have no known competing financial interests or personal relationships that could have appeared to influence the work reported in this paper.

#### Acknowledgment

This work was supported by Ministry-of-Education Key Laboratory for the Synthesis and Application of Organic Function Molecules, Hubei University.

#### References

- [1] A.T. Lima, A. Hofmann, D. Reynolds, C.J. Ptacek, P.V. Cappellen, L.M. Ottosen, S. Pamukcu, A. Alshawabek, D.M. O'Carroll, C. Riis, E. Cox, D.B. Gent, R. Landis, J. Wang, A.I.A. Chowdhury, E.L. Secord, A.S. Hachair, Environmental Electrokinetics for a sustainable subsurface, *Chemosphere*, 181 (2017) 122–133.
- [2] K. Legrouri, E. Khouya, H. Hannache, M. El Harti, M. Ezzine, R. Naslain, Activated carbon from molasses efficiency for Cr(VI), Pb(II) and Cu(II) adsorption: a mechanistic study, *Chem. Ind.*, 3 (2017) 301–310.
- [3] K. McCausland, R.C. Lobo, J. Hallett, J. Bates, B. Donovan, L.A. Selvey, It is stigma that makes my work dangerous: experiences and consequences of disclosure, stigma and discrimination among sex workers in Western Australia, *Cult. Health Sex*, 1390 (2020) 180–195.
- [4] L. Wei, Y. Li, H. Ye, J. Xiao, C. Hogstrand, I. Green, Z. Guo, D. Han, Dietary trivalent chromium exposure up-regulates lipid metabolism in coral trout: the evidence from transcriptome analysis, *Front. Physiol.*, 12 (2021) 640898, doi: 10.3389/fphys.2021.640898.
- [5] M. Iqbal, M. Abbas, J. Nisar, A. Nazir, A.Z. Qamar, Bioassays based on higher plants as excellent dosimeters for ecotoxicity monitoring: a review, *Chem. Int.*, 5 (2019) 1–80.
- [6] Y.A.B. Neolaka, Y. Lawa, J.N. Naat, A.A.P. Riwu, M. Iqbal, H. Darmokoesoemo, H.S. Kusuma, The adsorption of Cr(VI) from water samples using graphene oxide-magnetic (GO-Fe<sub>3</sub>O<sub>4</sub>) synthesized from natural cellulose-based graphite (kusambi wood or *Schleichera oleosa*): study of kinetics, isotherms and thermodynamics, *J. Mater. Res. Technol.*, 9 (2020) 6544–6556.
- [7] H. Gu, Y. Zhu, T. Jia, X. Li, Y.B. Lu, K. Kaku, Development of a new eczema-like reconstructed skin equivalent for testing child atopic dermatitis-relieving cosmetics, *J. Cosmet. Dermatol.-US*, 19 (2020) 752–757.
- [8] M.W. Yasir, M.B.A. Siddique, Z. Shabbir, H. Ullah, L. Riaz, Waqar-Un-Nisa, Shafeeq-ur-rahman, A.A. Shah, Biotreatment potential of co-contaminants hexavalent chromium and polychlorinated biphenyls in industrial wastewater: individual and simultaneous prospects, *Sci. Total Environ.*, 799 (2021) 146345, doi: 10.1016/j.scitotenv.2021.146345.
- [9] Y.S. Hedberg, Chromium and leather: a review on the chemistry of relevance for allergic contact dermatitis to chromium, *J. Leather Sci. Eng.*, 2 (2020), doi: 10.1186/s42825-020-00027-y.
- [10] M. Abbas, M. Adil, S. Ehtisham-ul-Haque, B. Munir, M. Yameen, A. Ghaffar, G.A. Shar, M. Asif Tahir, M. Iqbal, *Vibrio fischeri* bioluminescence inhibition assay for ecotoxicity assessment: a review, *Sci. Total Environ.*, 626 (2018) 1295–1309.
- [11] Y.S. Hedberg, Z. Wei, M. Matura, High release of hexavalent chromium into artificial sweat in a case of leather shoe-induced contact dermatitis, *Contact Derm.*, 82 (2020) 179–181.
- [12] Y. Yan, L. Li, The adsorption performance of hexavalent chromium Cr(VI) in aqueous with three biomass carbons materials, *IOP Conf. Ser.: Earth Environ. Sci.*, 615 (2020) 012115, doi: 10.1088/1755-1315/615/1/012115.
- [13] M. Axel, S. Michael, R. Bernd, Urine tropenol ester levels in workers handling tiotropium bromide synthesis: implications for exposure prevention and biomonitoring, *Arh Hig Rada Toksiko*, 70 (2020) 118–122.
- [14] J. Kobayashi, T. Minamizuka, M. Koshizaka, Y. Maezawa, H. Ono, K. Yokote, Serum HDL-C values: an extremely useful marker for differentiating homozygous lipoprotein lipase deficiency from severe hypertriglyceridemia with other causes in Japan, *Clin. Chim. Acta*, 521 (2021) 85–89.
- [15] D. Gutschmidt, A. Vera, Organizational culture, stress, and coping strategies in the police: an empirical investigation, *Police Pract. Res.*, 4 (2021) 507–522.
- [16] F. Minas, B.S. Chandravanshi, S. Leta, Chemical precipitation method for chromium removal and its recovery from tannery wastewater in Ethiopia, *Chem. Int.*, 3 (2017) 392–405.
- [17] Y.A.B. Neolaka, Y. Lawa, J. Naat, A.A.P. Riwu, A.W. Mango, H. Darmokoesoemo, B.A. Widyaningrum, M. Iqbal, H.S. Kusuma, Efficiency of activated natural zeolite-based magnetic composite (ANZ-Fe<sub>3</sub>O<sub>4</sub>) as a novel adsorbent for removal of Cr(VI) from wastewater, *J. Mater. Res. Technol.*, 18 (2022) 2896–2909.
- [18] S. Ata, A. Tabassum, I. Bibi, S. Ghafoor, A. Ahad, M.A. Bhatti, A. Islam, H. Rizvi, M. Iqbal, Synthesis and characterization of ZnO nanorods as an adsorbent for Cr(VI) sequestration, *Z. Phys. Chem.*, 233 (2019) 995–1017.
- [19] I.A. Bhatti, N. Ahmad, N. Iqbal, M. Zahid, M. Iqbal, Chromium adsorption using waste tire and conditions optimization by response surface methodology, *J. Environ. Chem. Eng.*, 5 (2017) 2740–2751.
- [20] M. Akram, H.N. Bhatti, M. Iqbal, S. Noreen, S. Sadaf, Biocomposite efficiency for Cr(VI) adsorption: kinetic, equilibrium and thermodynamics studies, *J. Environ. Chem. Eng.*, 5 (2017) 400–411.
- [21] T. Li, J. Yu, H. Sui, T. Zhang, R.H. Zhou, Bovine serum albumin-directed fabrication of nanohydroxyapatite with improved stability and biocompatibility, *Int. J. Nanosci.*, 20 (2021) 21500289, doi: 10.1142/S0219581X21500289.
- [22] A. Nayak, B. Bhushan, S. Kotnala, Fabrication of chitosan-hydroxyapatite nano-adsorbent for removal of norfloxacin from water: isotherm and kinetic studies, *Mater. Today: Proc.*, 61 (2022) 143–149.
- [23] C. Wang, R. Wu, J. Guo, Y. Cui, Effects of Cr(VI)-reducing bacteria on the behaviour of Cr(VI) adsorption by goethite and haematite: speciation and distribution, *J. Soils Sediments*, 20 (2020) 3733–3741.
- [24] W. Jia, J. Du, M. Jiang, M.Y. Zhang, E.L. Han, H.Q. Niu, D.Z. Wu, Preparation and Cr(VI) adsorption of functionalized polyimide fibers, *J. Appl. Polym. Sci.*, 139 (2022) 52799, doi: 10.1002/app.52799.

- [25] M. Agheli, A. Habibolahzadeh, Study of hexavalent chromium ion adsorption on nano-porous anodic aluminum oxide, *Prot. Met. Phys. Chem.*, 52 (2016) 972–974.
- [26] M. Ackmez, S. Mika, Magnetic nano-adsorbents for micropollutant removal in real water treatment: a review, *Environ. Chem. Lett.*, 19 (2021) 4393–4413.
- [27] R. Naveed, I.A. Bhatti, I. Sohail, A. Ashar, S.M. Ibrahim, M. Iqbal, A. Nazir, Kinetic and equilibrium study of (poly amido amine) PAMAM dendrimers for the removal of chromium from tannery wastewater, *Z. Phys. Chem.*, 235 (2020), doi: 10.1515/zpch-2019-1567.
- [28] J.M. Abdul, S. Vigneswaran, W.G. Shim, J. Kandasamy, Removal of metsulfuron methyl by granular activated carbon adsorption, *Desal. Water Treat.*, 21 (2010) 247–254.
- [29] S. Shindin, N. Parumasur, G. Lukumon, Numerical analysis of Fourier pseudospectral methods for the Klein–Gordon equation with smooth potentials, *Afr. Mat.*, 33 (2022), doi: 10.1007/s13370-022-01021-9.
- [30] J.C. Soares, A.C. Soares, P.A.R. Pereira, V.C. Rodrigues, F.M. Shimizu, M.E. Melendez, C.S. Neto, A.L. Carvalho, F. L. Leite, S.A.S. Machado, O.N. Oliveira, Adsorption according to the Langmuir – Freundlich model is the detection mechanism of the antigen p53 for early diagnosis of cancer, *Phys. Chem. Chem. Phys.*, 18 (2016) 8412–8418.